energies

MDPI

Article

Microscopic Mechanism for the Displacement of Shale Oil by CO_2 in Organic Nanopores

Xiangji Dou [1], Pengfei Zhu [1], Guodong Qi [2], Yanfeng He [1], Dongdong Shao [1] and Kun Qian [1,*]

[1] School of Petroleum and Natural Gas Engineering, Changzhou University, Changzhou 213164, China
[2] Jiangsu Oilfield Company, Sinopec Group, Yangzhou 225000, China
* Correspondence: qiankun@cczu.edu.cn

Abstract: The effective displacement of the shale oil from organic nanopores plays a significant role in development of the shale oil reservoirs. In order to deeply understand the microscopic displacement mechanism of alkane of shale oil by CO_2 in organic nanopores, microscopic pore model of organic matter and molecular model of CO_2 and n-dodecane were established to investigate the influences of key parameters on the displacement process by using the Monte Carlo and molecular dynamics simulation method. The instantaneous adsorption of molecules demonstrates that the displacement of n-dodecane and the adsorption of CO_2 are proportional to the increase of the injection pressure of CO_2 as well as the pore size. In addition, the results also show that the adsorption capacity of CO_2 first increases and then decreases with the increase of the temperature, which indicates that the optimum temperature exists for the adsorption of CO_2. This work can provide critical insights into understanding the microscopic displacement mechanism of shale oil by CO_2 in organic nanopores in shale oil reservoirs and lay a solid foundation for the CO_2 flooding in the shale oil reservoir and the CO_2 storage.

Keywords: shale oil; n-dodecane; CO_2; molecular dynamics simulation; displacement

Citation: Dou, X.; Zhu, P.; Qi, G.; He, Y.; Shao, D.; Qian, K. Microscopic Mechanism for the Displacement of Shale Oil by CO_2 in Organic Nanopores. *Energies* **2022**, *15*, 7064. https://doi.org/10.3390/en15197064

Academic Editor: Reza Rezaee

Received: 5 September 2022
Accepted: 22 September 2022
Published: 26 September 2022

1. Introduction

With the increasing demand for energy in the world and the gradual depletion of conventional oil and gas resources, it is an inevitable trend to seek another unconventional alternative energy in the future. Generally, shale oil is a very typical unconventional resource, and thus can be regarded as an important alternative energy source [1–3].

During the six periods of Early Silurian, Late Devonian, Late Carboniferous to Early Permian, Late Jurassic, Cretaceous, and Oligocene-Miocene, shale was widely deposited worldwide. During the formation period of the four sets of shale strata, the Upper Jurassic, Oligocene-Miocene, Cretaceous and Upper Devonian, the global temperature and humidity were relatively high, which was favorable for the formation and preservation of type I–II organic matter. The oil is mainly enriched in these layers, accounting for 87.83% of the total resources [3].

In recent years, shale oil is increasingly playing an important role in the energy supply, and then the adsorption and resolution of shale oil in nanopores has drawn extensive attention [4,5].Wang et al. [6] employed molecular dynamics (MD) simulation to study adsorption behavior of shale oil within nanoscale carbonaceous slits in shale system and they found that the adsorption portion of liquid n-alkanes always consists of multimolecular layers, and the thickness of each layer is approximately 0.48 nm under shale reservoir conditions. Based on N_2 and CO_2 composited adsorption isotherms, Wang et al. [7] established a simplified pillar-layer model to investigate CH_4 adsorption behavior and competitive adsorption effect between CO_2 and CH_4 and they concluded that CO_2 has stronger competitive adsorption ability than CH_4. Pang et al. [5] employed the experimental and analytical method to investigate the gas adsorption in organic nanopores and they

insisted that the gas adsorption decreased greatly in organic nanopores due to the effect of the moisture. Lately, Hazra et al. [8] used the low-pressure adsorption techniques to study the adsorption-desorption isotherms of the organic-rich Permian shales and they indicated that a strong positive relationship may be exist between the pore radius and the difference in volumes of gas. Memon et al. [9] adopted two supercritical CO_2 fracturing tests and low-pressure N_2 adsorption experiments to stimulate the supercritical CO_2-shale interactions during fracturing and they concluded that adsorption swelling can make the reduction of fracture aperture. The topics of the above literature mainly focus on the adsorption and resolution of shale oil in nanopores, the displacement of the shale oil from organic nanopores or inorganic nanopores by CO_2 is not taken into consideration.

The displacement of the shale oil from organic nanopores or inorganic nanopores by CO_2 has been extensively studied by many researchers [10–12]. Severson et al. [13] employed Monte Carlo method to study the effects of temperature and the length of carbon chain on the adsorption properties of alkanes in nanopores and found that the adsorption of alkanes with long-chain at high temperature is similar to that of alkanes with short-chain at low temperature. Lately, Pathak et al. [14] presented the adsorption and desorption of methane and CO_2 in methane-CO_2-kerogen system and concluded that CO_2 can effectively displace shale gas trapped in shale nanopores. Wang et al. [15] studied the storage morphology of linear alkanes in nanopores formed from organic by molecular dynamics simulation, and suggested that several adsorption layers of alkanes exist on the surface of nanopores and the thickness of the adsorption layer is about 0.42 nm. However, in the above literature, the effects of temperature, pore size, pressure and other comprehensive conditions on the adsorption mechanism in organic nanopores of shale reservoir are not studied. Recently, Haghshenas et al. [16] proposed the compositional simulation model to study the effect of fluid component adsorption on the displacement of oil by the CO_2 huff-n-puff performance and they concluded that the lower saturation pressure may be better to obtain the better results than that with the higher saturation pressure fluid. Liu et al. [17] used the molecular simulations to investigate the competitive adsorption behavior of hydrocarbon(s)/CO_2 mixtures in a double-nanopore system and they concluded that the CH_4 will be easily adsorbed in nanopores as the decrease of the pressure due to the stronger adsorption capacity of CO_2 on organic pore surface. Zhu et al. [18] conducted an experiment to illustrate the effect of different factors (such as shale properties, n-alkanes type and temperature) on the adsorption and dissolution behaviors of CO_2 and n-alkane mixtures in shale reservoirs. The above study of Liu et al. [17] and Zhu et al. [18] provided a guideline for quantitatively characterizing the effect of the injection pressure of CO_2 on the displacement of shale oil in this work.

To further analyze the effect of the injection pressure of CO_2, pore size and temperature on the displacing process of shale oil by CO_2, Grand Canonical Monte Carlo method and molecular dynamics method are employed to construct the graphene pore model with a vacuum layer. Based on that, the displacement of typical alkanes and the adsorption capacity of CO_2 are further discussed in detail. In addition, the optimum injection pressure of CO_2, pore size and temperature for the displacement of shale oil by CO_2 are determined, which can provide a new idea for the CO_2 flooding in the shale oil reservoir and the CO_2 storage.

2. Simulation System

2.1. Model Construction

(1) Single crystal cell structure of graphene was imported from the database of Materials Studio and thus the Graphene monolayer lamellae can be constructed. Then the pores-vacuum layers and supercell graphene pore model was built by the Super Cell in the database of Materials Studio respectively.

(2) In pores of graphene, n-dodecane molecular are injected and the force field of n-dodecane was distributed by the Dreiding force field [19,20]. Subsequently, Atom Based was used to obtain the sum method of Van der Waals' force and the electrostatic

force in isochoric-isothermal ensemble (NVT). And then, the simulations are run by periodic boundary. The schematic for the pore structure of n-dodecane adsorbed is shown in Figure 1.

(3) The pre-adsorption simulation of n-dodecane molecules in graphene pores was further conducted to obtain the stable adsorption configuration of n-dodecane. After that, CO_2 molecules with different injection pressures were added into the pore model to simulate and study the dynamic displacing process of n-dodecane molecules by CO_2 [21,22].

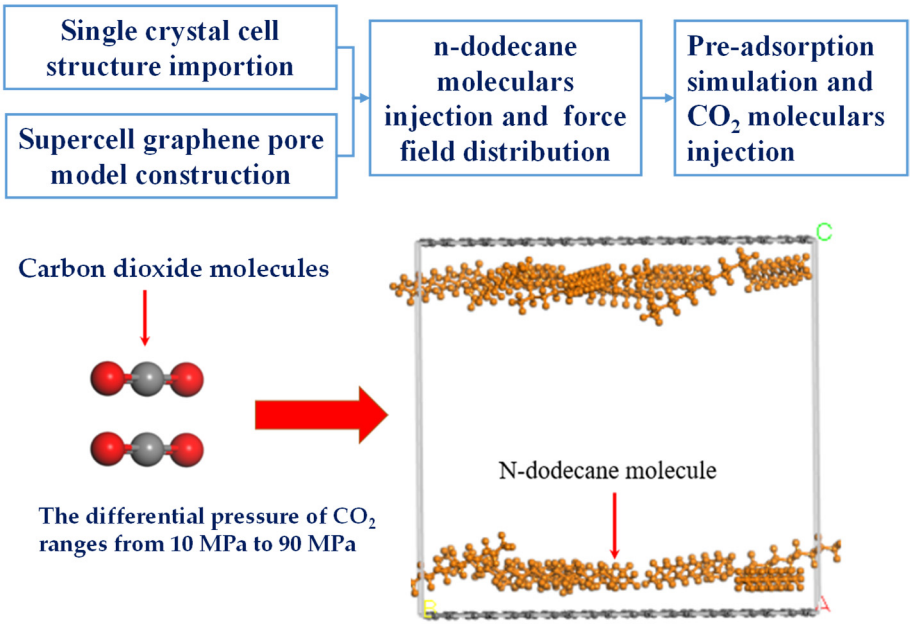

Figure 1. Schematic diagram of n-dodecane adsorbed in pores under different injection pressures of CO_2. (A, B and C respectively represent different coordinate directions).

2.2. Optimization of Computational Model

Before the displacing simulation, structural model of graphene, CO_2 molecular model and n-dodecane molecular model should be optimized to obtain the energy minimization. Based on that, the optimized models are employed to conduct the molecular simulation [23]. The optimization steps of the computational models (including the structural model of graphene, CO_2 molecular model and n-dodecane molecular model) are as follows:

(4) The SMART option in Task Geometry Optimization under the Forcite module of Molecular Dynamics was selected to optimize the geometry of the constructed model, and then the stable graphene slit structure was obtained;

(5) The COMPASS force filed was selected to stimulate the force field and the sum method of Atom based was used to obtain the Van der Waals' force;

(6) The optimization of CO_2 molecular model and n-dodecane molecular model are similar to that of the structural model of graphene.

2.3. Calculation Method

Generally, the adsorption and free states of CO_2 and n-dodecane molecules in graphene pores are based on the interactional force between atoms and molecules. In this work, L-J potential energy model is adopted to analyze the potential energy between molecules and the potential energy of each molecule is listed in Table 1. Meanwhile, to describe the Van der Waals' force in the system, the following potential-energy function is employed,

$$U(ij) = 4\varepsilon_{ij}[(\frac{\sigma_{ij}}{r_{ij}})^{12} - (\frac{\sigma_{ij}}{r_{ij}})^{6}] + \frac{q^i q^j}{r_{ij}} \quad (1)$$

where r_{ij} represents the distance between the i-th particle and the j-th particle. q^i and q^j are the electric charge of i-th particle and j-th particle, respectively. ε is the the energy action parameter and σ is the dimensional action parameter.

Table 1. L-J potential energy of each molecule used in this work.

Site	σ/nm	(ε/K_B)/K
CO_2	0.363	242.0
C (CNT)	0.350	35.26
$C_{12}H_{26}$	0.785	715

2.4. Modeling Scheme

In this work, to simulate the dynamic displacing process of shale oil by CO_2 in pores of graphene, the long chain atom model and three-point hard-sphere linear model are used to represent n-dodecane molecule and CO_2 molecule, respectively. Meanwhile, the interactional forces between the CO_2 molecule, n-dodecane molecule and graphene slits are calculated by the L-J potential energy model. In order to simulate the effect of CO_2 displacing shale oil under different injection pressure of CO_2, different pore size and different temperature, Grand Canonical Monte Carlo (GCMC) method is further used. The simulation steps are as follows:

(1) n-dodecane molecules must be adsorbed in pores of graphene in advance, and the adsorption capacity of n-dodecane molecules depends on the differential pressure of n-dodecane;
(2) CO_2 molecules with differential pressures are injected into organic nanopores that reached stable adsorption state. And when the adsorption of CO_2 reached equilibrium state in pores, the injection of CO_2 should be stopped immediately;
(3) The displacement capacity of n-dodecane and the adsorption capacity of CO_2 in pores are calculated when the adsorption equilibrium state is obtained;
(4) Through the above simulation steps, single factor control variate method can be adopted to analyze the effects of injection pressure of CO_2, pore size and temperature on the displacement of n-dodecane and the adsorption of CO_2.

3. Results and Discussion

In this section, the effects of some parameters, such as the injection pressure of CO_2, pore size and temperature, on the displacement of shale oil by CO_2 are discussed in detail.

3.1. Injection Pressure of CO_2

In order to investigate the effect of the injection pressure of CO_2 on the displacement of shale oil, the molecular simulation process of this section is as follows,

(1) The pore size of the pore model is fixed at 40 Å and the simulated temperature is set at 373 K and the differential pressure of n-dodecane is set at 30 MPa;
(2) Before the molecular simulation, n-dodecane should be adsorbed on the pore wall in advance. After that, CO_2 is injected into the pore and the injection pressure of CO_2 gradually increases from 0 MPa to 90 MPa;
(3) When the dynamic displacing process reached equilibrium, the displacement of n-dodecane and the adsorption of CO_2 were further analyzed with the increase of the injection pressure of CO_2.

Figures 2–4 mainly show the instantaneous adsorption of molecules under the injection pressure of CO_2 at 0 MPa, 50 MPa and 90 MPa, respectively. In order to calculate the displacement of shale oil, the following equation is employed,

$$N_d = N_t - N_p \quad (2)$$

where N_d is the number of n-dodecane molecules displaced by CO_2. N_t is number of n-dodecane molecules absorbed in the pores when the injection pressure of CO_2 is 0 MPa. N_p is the number of n-dodecane molecules absorbed in the pores under differential CO_2 injection pressures.

In Figure 2a, the yellow spheres represent n-dodecane molecules, and the red and gray spheres are carbon dioxide molecules. As can be seen from Figure 2a, carbon dioxide molecules cannot be naturally adsorbed into pores, in which are fully absorbed by n-dodecane molecules in the surface of pores. When the injection pressure of CO_2 increases to some degree (such as 50 MPa, shown in Figure 2b), some n-dodecane molecules gradually enter into pores while some carbon dioxide molecules absorbed in the surface of pores tend to desorb and become free-state at the same time. When the injection pressure of CO_2 increases to 90 MPa (shown in Figure 2c), n-dodecane molecules completely desorb from pores and become free state, while at the same time, the surface of pores is almost absorbed by carbon dioxide molecules, which indicates that the adsorption capacity of CO_2 is much stronger than that of n-dodecane under reservoir conditions and the adsorbed shale oil can be fully displaced by CO_2 when the injection pressure of CO_2 is large enough.

Based on Equation (2), the displacement of n-dodecane and the adsorption of CO_2 can be calculated, shown in Figure 3. As can be seen from Figure 3, the displacement of n-dodecane can be more sensitive when the injection pressure of CO_2 is smaller than 60 MPa. Taking relation between the displacement of n-dodecane and the injection pressure of CO_2 as an example, when the injection pressure of CO_2 increases from 10 MPa to 40 MPa, the displacement of n-dodecane accordingly increase from 13.93 mol/uc to 48.93 mol/uc with an increasing ratio of 251.26%. When the injection pressure of CO_2 increases from 60 MPa to 90 MPa, the increasing ratio is only 9.69%. This phenomenon indicates that the absorbed shale oil is mainly displaced when the injection pressure of CO_2 is smaller than 60 MPa. Meanwhile, when the injection pressure of CO_2 is less than 20 MPa, the adsorption of CO_2 rises sharply as the increase of the injection pressure. For instance, the adsorption of CO_2 rises from 368.36 mol/uc to 488.65 mol/uc with an increasing ratio of 32.66% when the injection pressure of CO_2 accordingly increases from 10 MPa to 20 MPa, while the increasing ratio is only 0.38% when the injection pressure of CO_2 increases from 80 MPa to 90 MPa. The underlying cause for this phenomenon may be that the interactional force between the carbon dioxide molecules and the surface of pores tends to increase with the growth of the injection pressure of CO_2. From the above phenomenon, we can conclude that the displacement of shale oil by CO_2 is positively correlated with the injection pressure of CO_2 and CO_2 can be stored in shale reservoirs when the injection pressure of CO_2 is larger than 20 MPa, which can provide new thought for carbon dioxide storage.

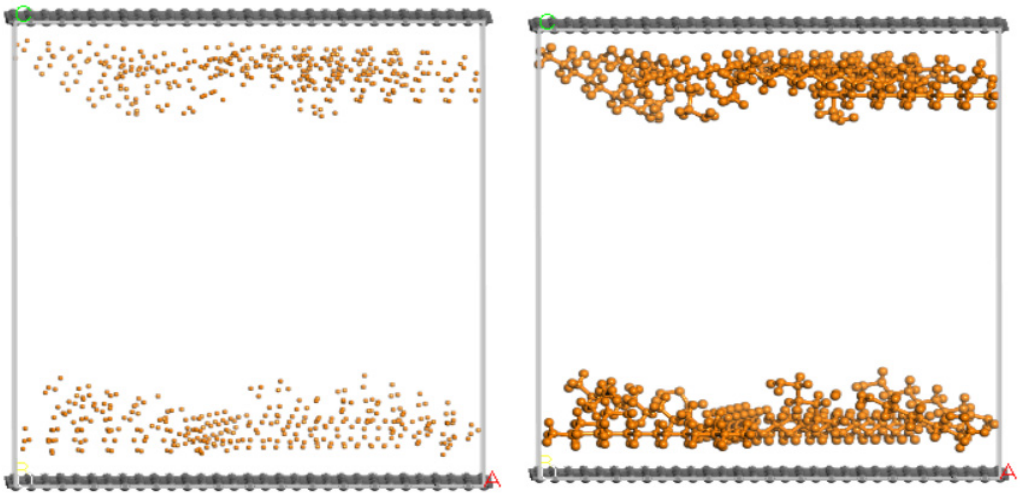

(**a**) P_{iCO2} = 0 MPa

Figure 2. *Cont.*

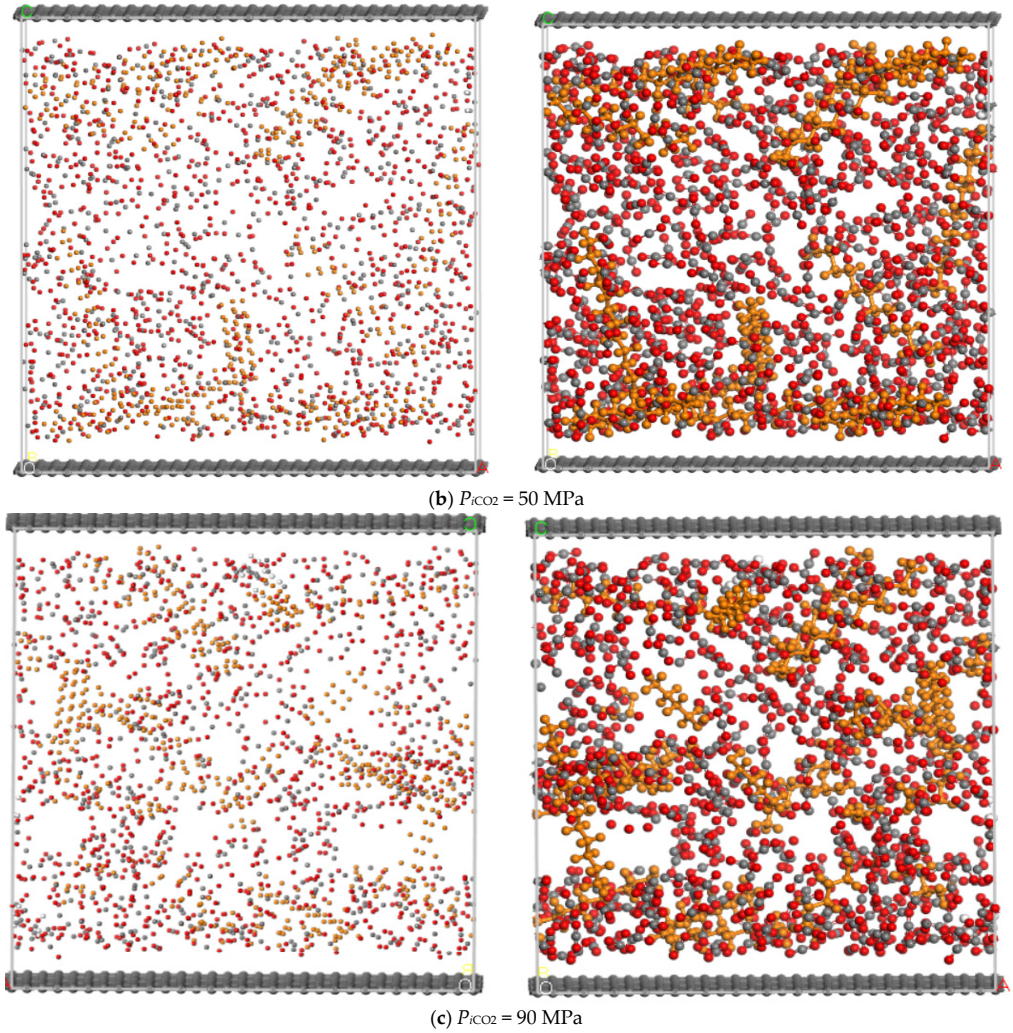

Figure 2. The schematic of instantaneous adsorption of molecules with CO_2 injection under different injection pressure. (A, B and C respectively represent different coordinate directions).

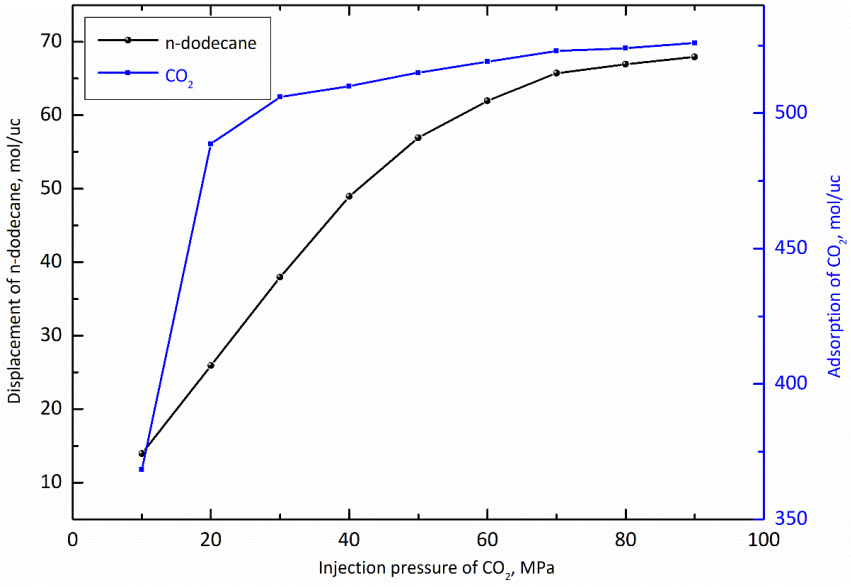

Figure 3. The molar quantity of n-dodecane displaced by CO_2 and the molar quantity of CO_2 absorbed in the pores at different injection pressure of CO_2.

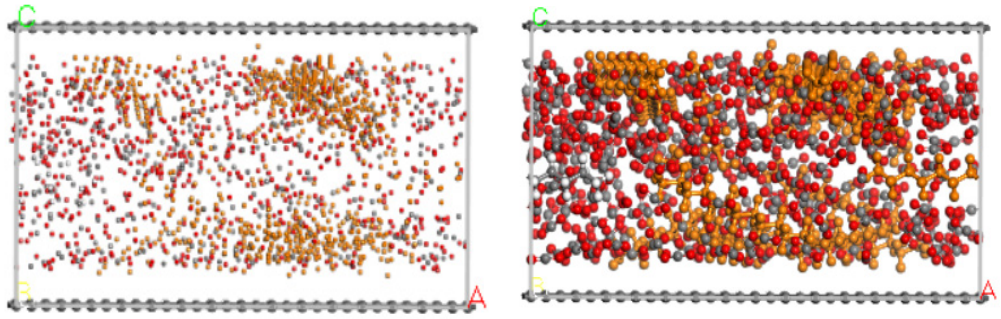

(**a**) P_{iCO2} = 60 MPa, 20 Å

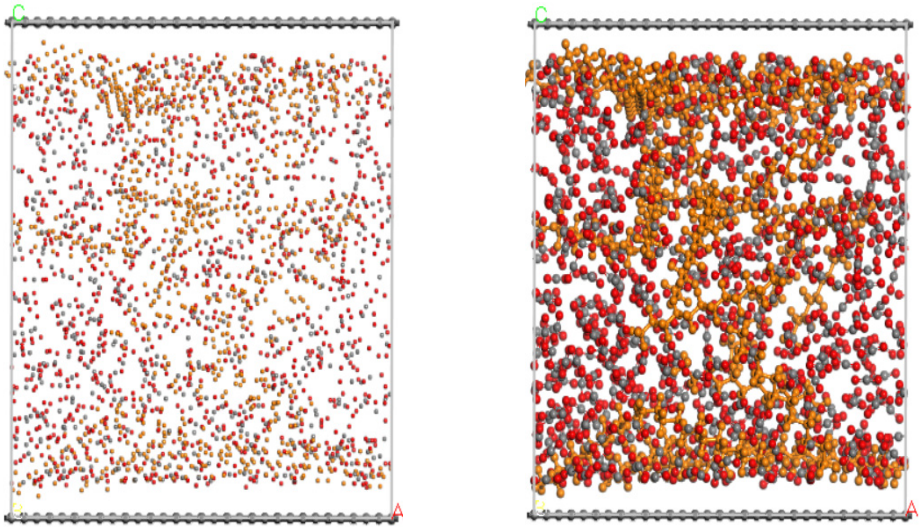

(**b**) P_{iCO2} = 60 MPa, 40 Å

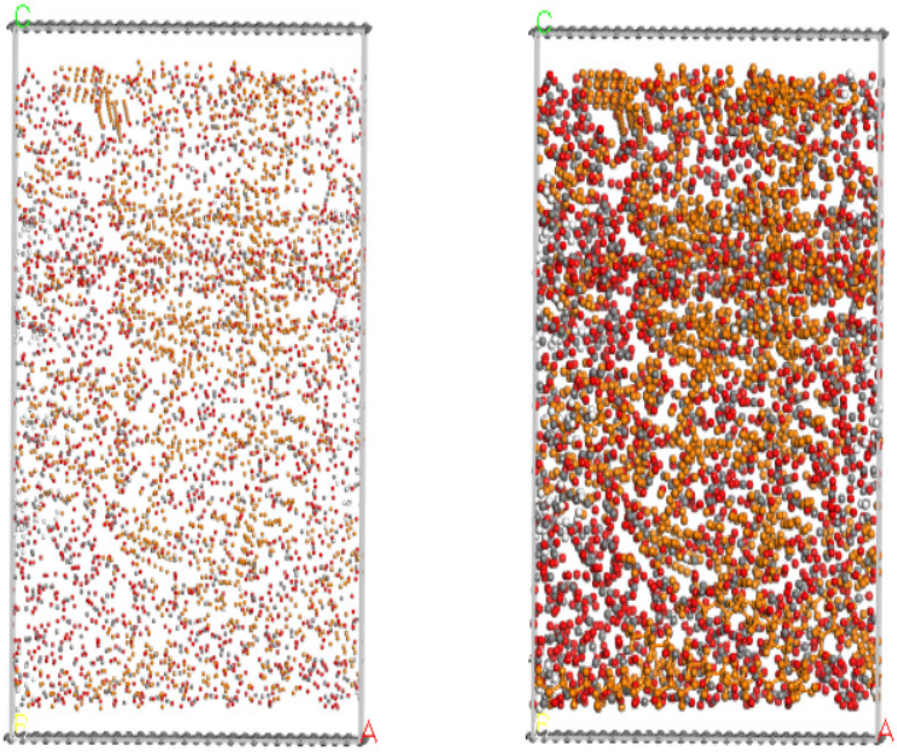

(**c**) P_{iCO2} = 60 MPa, 60 Å

Figure 4. The schematic of instantaneous adsorption of molecules with CO_2 injection under 60 MPa in pores of different sizes. (A, B and C respectively represent different coordinate directions).

3.2. Pore Size

In order to comprehensively investigate the influence of the pore size on the displacement of shale oil by CO_2, the pore size ranges from 20 Å to 60 Å and the instantaneous adsorption of molecules are displayed in Figure 4. Meanwhile, the displacing process of n-dodecane is assumed to be constant temperature to avoid the influence of temperature (T = 373 K). Generally, reservoir pressure plays a significant role in the adsorption of n-dodecane in pores and thus we should study the influence of pore size on the adsorption of n-dodecane under different reservoir pressures, shown in Figure 5.

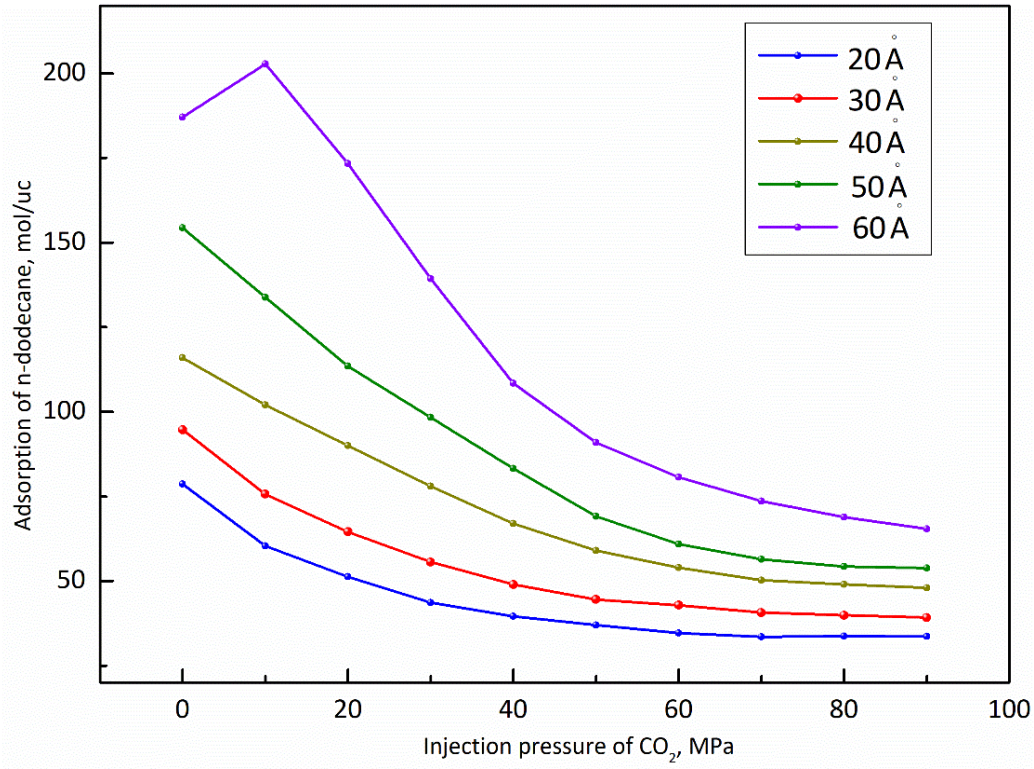

Figure 5. The molar quantity of n-dodecane absorbed in the pores of different sizes under different injection pressure of CO_2.

It can be seen from Figure 4, adsorption layers exist on the surface of pores while the thickness of adsorption layers are significantly various when the pore size is different. Generally, the adsorption of molecules in the surface of pores increases exponentially with the increase of the pore size and thus the thickness of adsorption layers will be greatly increased. This phenomenon can be explained by that with the increase of the pore size, the interaction between molecules gradually increases, and the molecular motion becomes more severe, which increases the probability of collision between n-dodecane molecules and pores. Meanwhile, due to the collision between n-dodecane molecules and pores, n-dodecane molecules will be desorbed from the surface of pores and accordingly CO_2 will be adsorbed into the corresponding pores.

As can be observed from Figure 5, the adsorption of n-dodecane is proportional to the pore size for a fixed injection pressure of CO_2. From Figure 5, we can find that the increase of the adsorption of n-dodecane is slightly different when the pore size has an equal increase. For example, at P_{iCO2} = 10 MPa, the adsorption of n-dodecane increases from 60.35 mol/uc to 75.66 mol/uc with an increasing ratio of 25.37% when the pore size accordingly increases from 20 Å to 30 Å while the increasing ratio can up to 51.53% if the pore size increases from 50 Å to 60 Å, which indicates that the larger the pore size is, the easier the adsorption of n-dodecane obtains. Meanwhile, as the increase of the injection pressure of CO_2, the increasing degree of n-dodecane tends to be weakened with

the increase of the pore size. For instance, at P_{iCO2} = 50 MPa, when the pore size increases from 20 Å to 30 Å, the increasing ratio of the adsorption of n-dodecane is only 20. 41% while under the same condition, the increasing ratio of the adsorption can up to 47.88% at P_{iCO2} = 20 MPa. In addition, when the pore size is fixed at 60 Å, the adsorption of n-dodecane increases first and then decrease with the increases of the injection pressure of CO_2, while for other cases, the adsorption of n-dodecane decreases with the increase of the injection pressure, shown in Figure 5. The underlying cause for this phenomenon may be that, for a pore large enough, the small amount of injected CO_2 has difficulty to move to the pore wall to displace adsorbed n-dodecane considering the great distances of CO_2 molecules to the wall. The total bulk pressure, including the bulk pressure of n-dodecane would be increased, which bring higher adsorption amount of n-dodecane. With injection pressure increasing, more CO_2 molecules appear in the pore, and there is higher opportunity to reach the pore wall to replace adsorbed n-dodecane. As a result, the adsorption of n-dodecane would decrease.

Generally, the displacement of shale oil by CO_2 always depends on the adsorption of CO_2 and thus the effect of the pore size on the adsorption of CO_2 should be discussed in detail, shown in Figure 6. As can be seen from Figure 6, when the pore size ranges from 20 Å to 50 Å, the increase of the adsorption capability of CO_2 becomes slowly with the increase of the pore size, while when the pore size increases from 50 Å to 60 Å, the adsorption capability of CO_2 increases rapidly. For example, at P_{iCO2} = 10 MPa, the adsorption capability of CO_2 increases from 312.66 mol/uc to 333.25 mol/uc with an increasing ratio of 6.59% when the pore size accordingly increases from 20 Å to 30 Å, while the increasing ratio can reach 22.64% when the pore size increases from 50 Å to 60 Å. This phenomenon implies that when the pore size of shale matrix reaches 60 Å by hydraulic fracturing or acid fracturing technology, the production of shale oil can increase dramatically due to the huge increase of the adsorption of CO_2. Meanwhile, when the injection pressure of CO_2 is greater than 20 MPa, the effect of the pore size on the adsorption of CO_2 tends to be stable, showing that the adsorption curves of different pore sizes are parallel to each other.

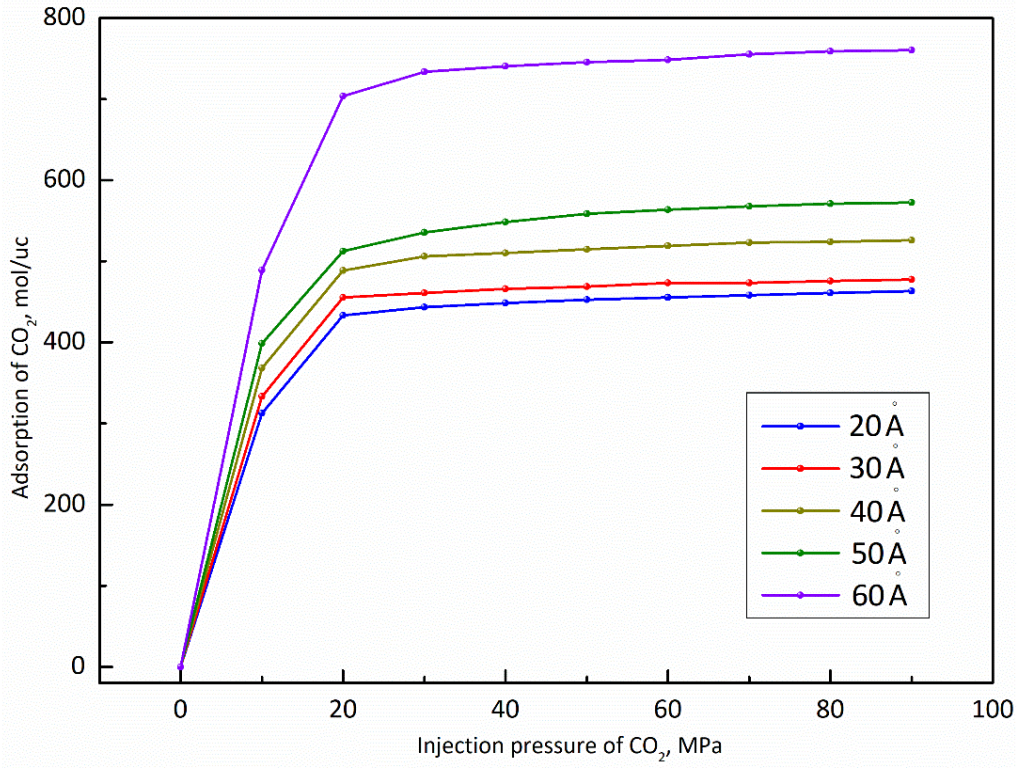

Figure 6. The molar quantity of CO_2 absorbed in the pores of different sizes under different injection pressure.

After that, the effect of the pore size on the displacement of n-dodecane under the CO_2 injection pressure of 60 MPa is discussed in Figure 7. As displayed in Figure 7, the displacement of n-dodecane increased with the increase of pore size, and the increasing degree tends to be strengthened when the pore size changes from 30 Å to 40 Å. The displacement capacity of n-dodecane increases from 43.97 mol/uc to 50.16 mol/uc when the pore size accordingly increases from 20 Å to 30 Å with an increasing ratio of 14.07%, while the increasing ratio is 43.38% when the pore size increases from 30 Å to 40 Å. From the above phenomenon, we can conclude that the larger the pore size is, the easier the displacement of shale oil by CO_2 is.

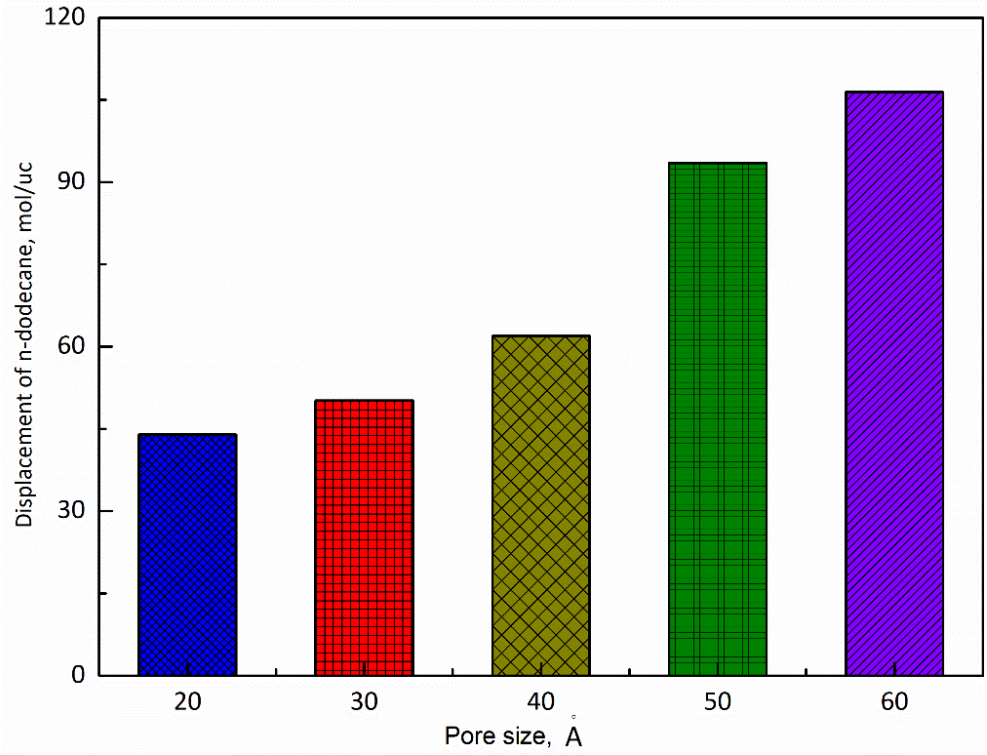

Figure 7. The molar quantity of n-dodecane displaced by CO_2 in the pores of different sizes under CO_2 injection pressure of 60 MPa.

3.3. Temperature

In this section, we mainly discuss the effect of temperature on the displacement of the shale oil by CO_2. In order to fully reveal the effect of the temperature on the displacement of the shale oil, the pore size of the pore model is fixed at 40 Å and the differential pressure is assumed to be equal to 30 MPa.

The displacement of n-dodecane by CO_2 at different temperatures can be visually observed by analyzing the instantaneous adsorption of molecules, shown in Figure 8. At T = 353 K (Figure 8b), the adsorption capacity of n-dodecane in the surface of pores is obviously smaller than that at T = 333 K (Figure 8a), while the adsorption capacity of n-dodecane is similar to that of CO_2. Further, when we compare the instantaneous adsorption at T = 373 K (Figure 8c) and the instantaneous adsorption at T = 393 K (Figure 8d), we can observe that the adsorption of CO_2 is dominant and n-dodecane exists in the free state in pores. In particular, as can be seen from Figure 8d (T = 393 K), only a small amount of n-dodecane is adsorbed into the surface of pores, which implies that n-dodecane molecular are almost displaced by CO_2 under the above situation. In addition, when the temperature is fixed at T = 413 K (Figure 8e), we can find that all n-dodecane molecular originally adsorbed in the surface of pores are completely displaced, which can be explained by that the higher the temperature is, the higher the kinetic energy is, and thus the displacement of n-dodecane by CO_2 is accelerated.

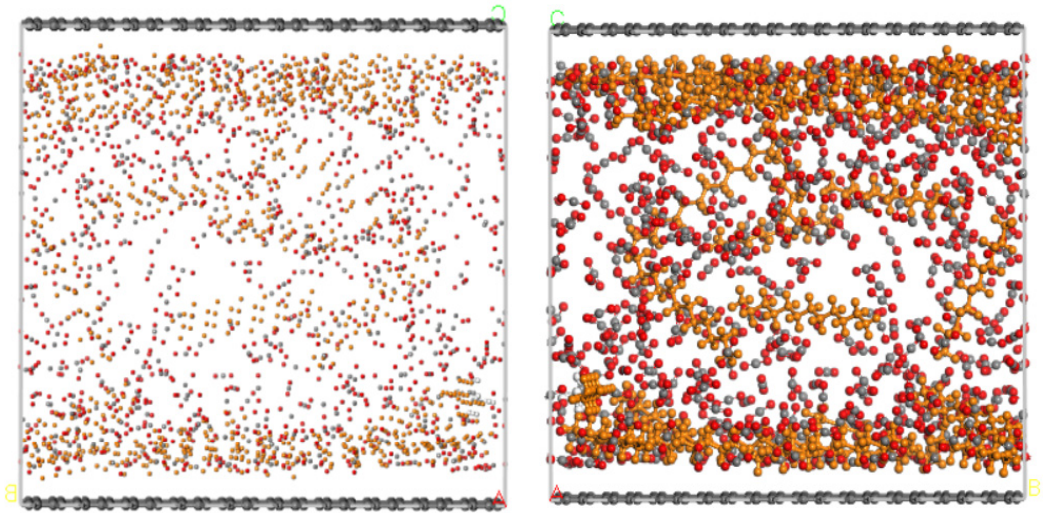

(**a**) P_{iCO2} = 60 MPa, T = 333 K

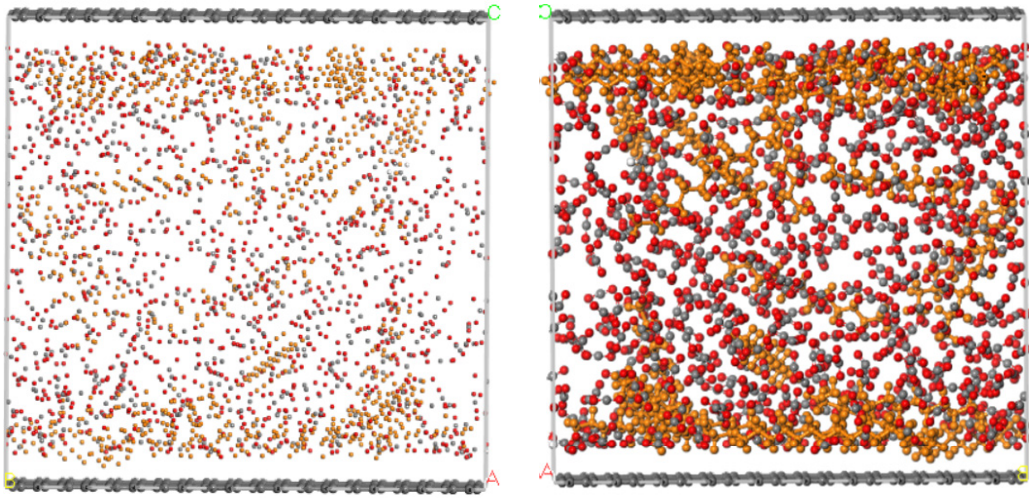

(**b**) P_{iCO2} = 60 MPa, T = 353 K

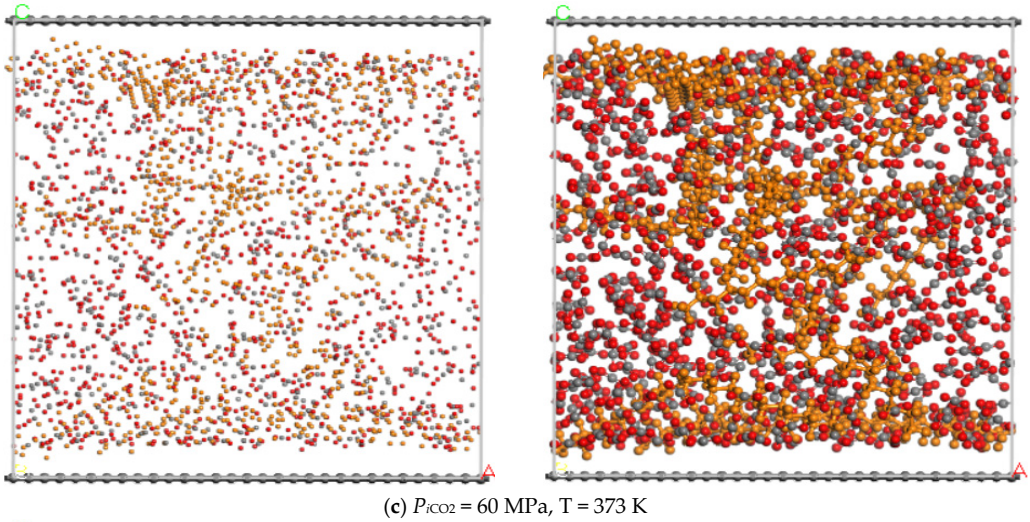

(**c**) P_{iCO2} = 60 MPa, T = 373 K

Figure 8. *Cont.*

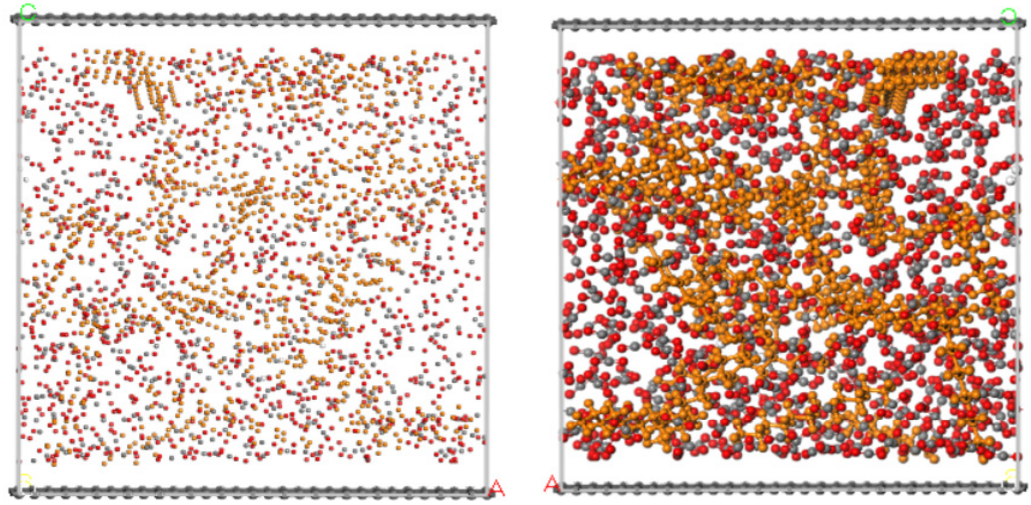

(**d**) P_{iCO2} = 60 MPa, T = 393 K

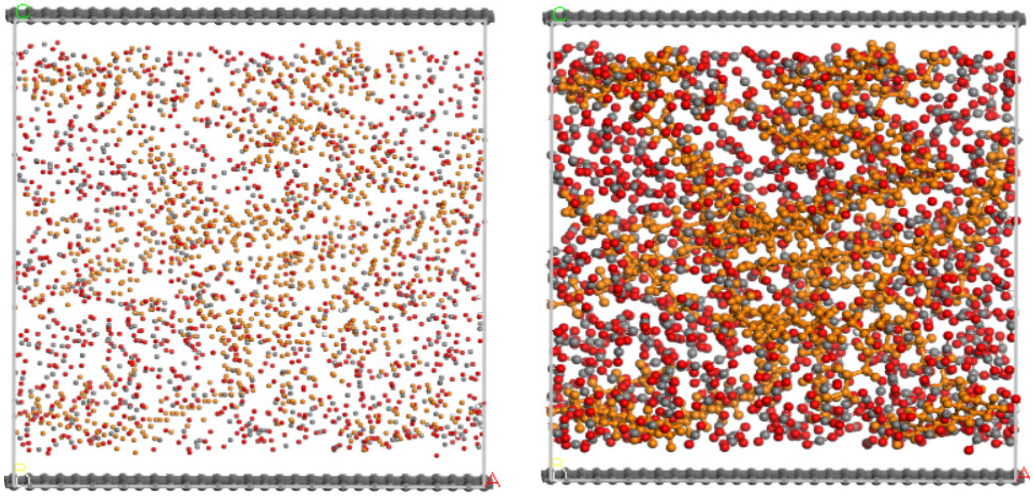

(**e**) P_{iCO2} = 60 MPa, T = 413 K

Figure 8. The schematic of instantaneous adsorption of molecules with CO_2 injection pressure of 60 MPa under different temperature. (A, B and C respectively represent different coordinate directions).

Similarly, Figure 9 mainly illustrates the effect of the temperature on the adsorption of n-dodecane and Figure 10 is on the influence of the temperature on the adsorption of CO_2. As can be seen from Figure 9, the temperature is conducive to the adsorption of n-dodecane, which can be explained by that the higher the temperature is, the less energy the n-dodecane molecular need to adsorb into the surface of pores. However, the influence of the temperature on the adsorption of n-dodecane tends to be weakened with the increase of the injection pressure. For example, at P_{iCO2} = 20 MPa, the adsorption capacity of n-dodecane decreases from 101 mol/uc to 90 mol/uc with a dropping ratio of 12.22% when the temperature decreases from 393 K to 373 K, while at P_{iCO2} = 70 MPa, the dropping ratio is only 9.52% under the same condition.

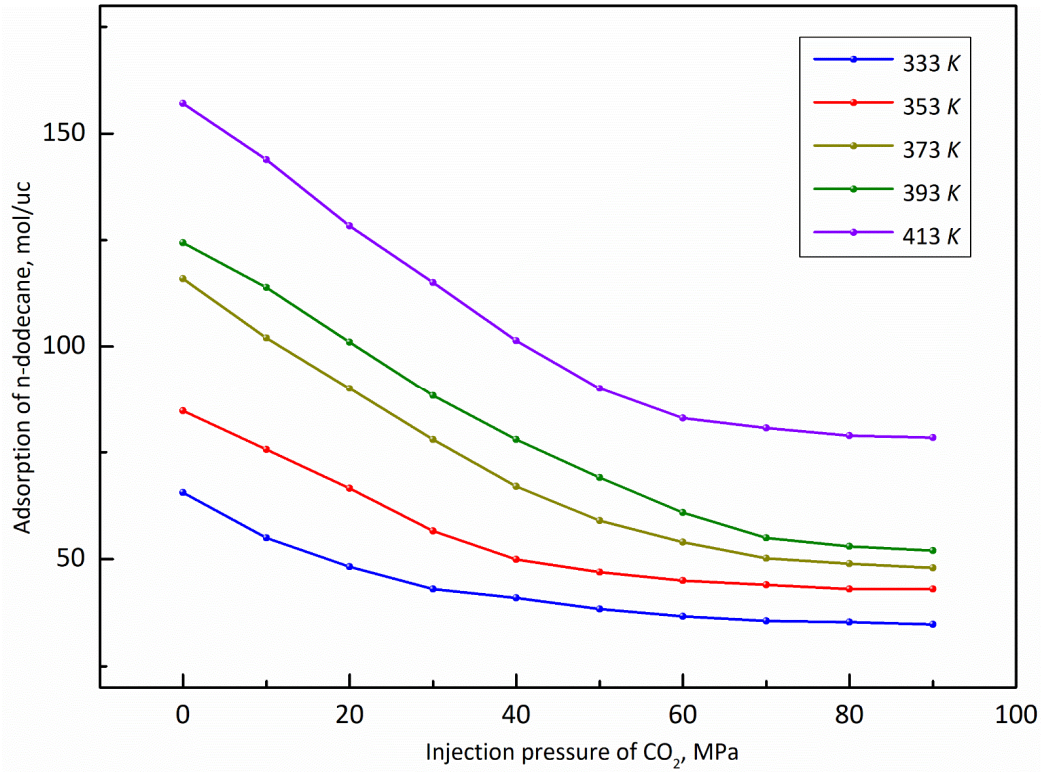

Figure 9. The molar quantity of n-dodecane absorbed in the pores under different temperature at different injection pressure of CO_2.

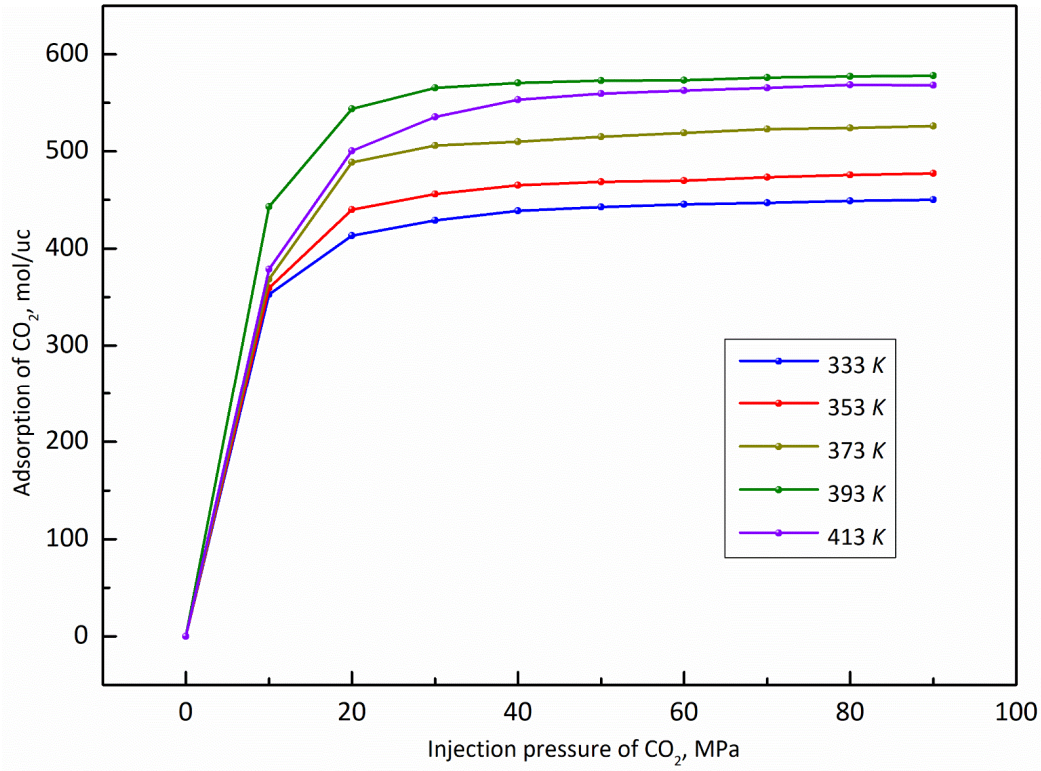

Figure 10. The molar quantity of CO_2 absorbed in the pores under different temperature at different injection pressure of CO_2.

From Figure 10, we can observe that when the temperature is lower than 393 K, the increase of the temperature is conductive to the adsorption of CO_2, while when the

temperature is above 393 K, the adsorption capacity of CO_2 will be slightly reduced, which indicates that the optimum temperature for the adsorption of CO_2 is 393 K. The underlying cause for this phenomenon may be that when the temperature is over 393 K, Brownian movement of CO_2 will be greatly enhanced and thus more energy is needed to make CO_2 adsorbed into the surface of pores. Meanwhile, the effect of temperature on the adsorption of CO_2 is various at different injection pressures. For example, at P_{iCO2} = 10 MPa, the adsorption capacity of CO_2 increases from 352.66 mol/uc to 368.36 mol/uc when the temperature accordingly increases from T = 333 K to T = 373 K with an increasing ratio of 4.45%, while at P_{iCO2} = 60 MPa, the increasing ratio can up to 16.47% under the same condition. This phenomenon indicates that the effect of temperature on the adsorption of CO_2 is more sensitive under medium-high injection pressure.

Further, the effect of the temperature on the displacement of n-dodecane is displayed in Figure 11. As illustrated in Figure 11, we can observe that the displacement capacity of n-dodecane by CO_2 is stronger at higher temperature. And, when the temperature of shale oil reservoir is lower than 373 K, the displacement capacity of n-dodecane increases dramatically. For instance, when the temperature increases from T = 333 K to T = 373 K, the displacement capacity of n-dodecane increases from 28.97 mol/uc to 60.42 mol/uc with an increasing ratio of 108.56%, while the increasing ratio is only 16.57 % when the temperature increases from T = 373 K to T = 413 K. Based on that phenomenon, we can conclude that there is an optimal temperature that the maximum displacement capacity of shale oil by CO_2 can be obtained from the perspective of economic production.

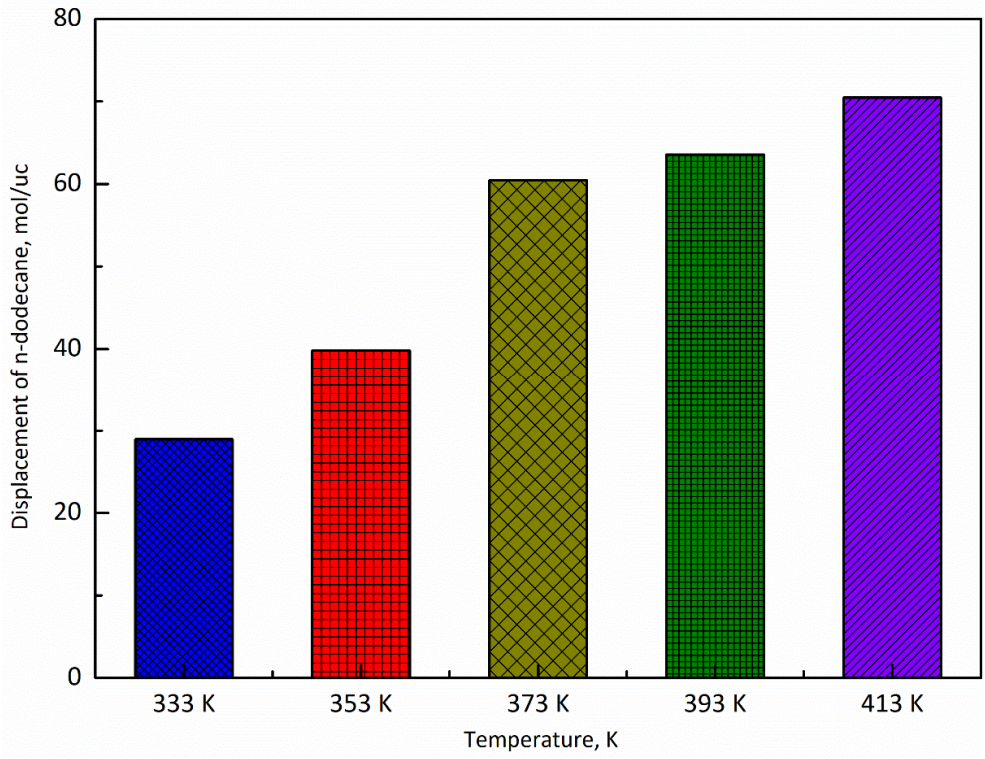

Figure 11. The molar quantity of n-dodecane displaced by CO_2 under different temperature at CO_2 injection pressure of 60 MPa.

4. Conclusions

In this work, Grand Canonical Monte Carlo and molecular dynamics methods are used to study the microscopic displacing process of n-dodecane by CO_2 in shale oil reservoirs. Based on the discussion on the displacement of n-dodecane and the adsorption capacity of CO_2 under different conditions, the following conclusions can be obtained:

(1) The adsorption capacity of CO_2 is much stronger than that of shale oil under reservoir conditions, which indicates that shale oil can be effectively displaced by CO_2. And,

the displacement capacity of shale oil by CO_2 and the adsorption capacity of CO_2 show a positive correlation with the injection pressure of CO_2.

(2) The larger the pore size, the stronger the capacity to store shale oil and the easier it is for CO_2 to displace the shale oil. Moreover, when the pore size ranges from 20 Å to 50 Å, the adsorption capacity of n-dodecane decreases with the the injection pressure of CO_2. When the pore size reaches 60 Å, the adsorption capacity of n-dodecane fist increases under pressure less than 10 MPa and then decreases as the pressure increases larger than 10 MPa.

(3) The adsorption capacity of CO_2 is highly sensitive to temperature. The adsorption capacity of CO_2 increases first and then decreases with the increase of the temperature and the highest adsorption capacity appeared at the temperature of 393 K, while the displacement capacity of n-dodecane increases with the increase of temperature. Overall, higher temperature is more favorable for the displacement of shale oil by CO_2.

Author Contributions: All authors have contributed to this work. X.D. conducted the molecular simulation and wrote the main manuscript. P.Z., G.Q., Y.H. and D.S. contributed to the modeling, drawing, and results analysis and discussion. K.Q. made substantial contributions to the conception/design of the work as the corresponding author. All authors have read and agreed to the published version of the manuscript.

Funding: This study was funded by the National Natural Science Foundation of China (Program No. 52004038), the Natural Science Research of Jiangsu Higher Education Institutions of China (Program No. 20KJB440003).

Data Availability Statement: All the data have been included in the manuscript.

Conflicts of Interest: The authors declare no conflict of interest.

Abbreviations

MD	molecular dynamics
NVT	isochoric-isothermal ensemble
CNT	carbon nanotube
GCMC	Grand Canonical Monte Carlo

References

1. Zhang, L.; Bao, Y.; Li, J.; Li, Z.; Zhu, R.; Zhang, J. Movability of lacustrine shale oil: A case study of Dongying Sag, Jiyang Depression, Bohai Bay Basin. *Pet. Explor. Dev.* **2014**, *41*, 703–711. [CrossRef]
2. Al-Mudhafar, W.J. Polynomial and nonparametric regressions for efficient predictive proxy metamodeling: Application through the CO_2-EOR in shale oil reservoirs. *J. Nat. Gas Sci. Eng.* **2019**, *72*, 103038. [CrossRef]
3. Yang, Z.; Bryant, S.; Dong, M. A method of determining adsorptive-gas permeability in shale cores with considering effect of dynamic adsorption on flow. *Fuel* **2020**, *268*, 117340. [CrossRef]
4. Wei, M.; Zhang, L.; Xiong, Y.; Li, J. Nanopore structure characterization for organic-rich shale using the non-local-density functional theory by a combination of N_2 and CO_2 adsorption. *Microporous Mesoporous Mater.* **2016**, *227*, 88–94. [CrossRef]
5. Pang, Y.; Soliman, M.Y.; Deng, H.; Xie, X. Experimental and analytical investigation of adsorption effects on shale gas transport in organic nanopores. *Fuel* **2017**, *199*, 272–288. [CrossRef]
6. Wang, S.; Feng, Q.H.; Javadpou, F.; Xia, T.; Li, Z. Oil adsorption in shale nanopores and its effect on recoverable oil-in-place. *Int. J. Coal Geol.* **2015**, *147–148*, 9–24. [CrossRef]
7. Wang, X.; Zhai, Z.; Jin, X.; Wu, S.; Li, J.; Sun, L.; Liu, X. Molecular simulation of CO_2/CH_4 competitive adsorption in organic matter pores in shale under certain geological conditions. *Pet. Explor. Dev.* **2016**, *43*, 841–848. [CrossRef]
8. Hazra, B.; Wood, D.A.; Vishal, V.; Varma, A.K.; Sakha, D.; Singh, A.K. Porosity controls and fractal disposition of organic-rich Permian shales using low-pressure adsorption techniques. *Fuel* **2018**, *220*, 837–848. [CrossRef]
9. Memon, S.; Feng, R.; Ali, M.; Bhatti, M.A.; Giwelli, A.; Keshavarz, A.; Xie, Q.; Sarmadivaleh, M. Supercritical CO_2-Shale interaction induced natural fracture closure: Implications for $scCO_2$ hydraulic fracturing in shales. *Fuel* **2022**, *313*, 122682. [CrossRef]
10. Al-Abri, A.; Hiwa, S.; Robert, A. Experimental investigation of the velocity-dependent relative permeability and sweep efficiency of supercritical CO_2 injection into gas condensate reservoirs. *J. Nat. Gas Sci. Eng.* **2009**, *1*, 158–164. [CrossRef]
11. Cao, Z.; Jiang, H.; Zeng, J.; Saibi, H.; Lu, T.; Xie, X.; Zhang, Y.; Zhou, G.; Wu, K.; Guo, J. Nanoscale liquid hydrocarbon adsorption on clay minerals: A molecular dynamics simulation of shale oils. *Chem. Eng. J.* **2021**, *420*, 127578. [CrossRef]

12. Dang, W.; Jiang, S.; Zhang, J.; Li, P.; Nie, H.; Liu, Y.; Li, F.; Sun, J.; Tao, J.; Shan, C.; et al. A systematic experimental and modeling study of water adsorption/desorption behavior in organic-rich shale with different particle sizes. *Chem. Eng. J.* **2021**, *426*, 130596. [CrossRef]
13. Severson, B.L.; Snurr, R.Q. Monte Carlo simulation of n-alkane adsorption isotherms in carbon slit pores. *J. Chem. Phys.* **2007**, *126*, 134708. [CrossRef] [PubMed]
14. Pathak, M.; Pawar, G.; Huang, H.; Deo, M.D. Carbon Dioxide Sequestration and Hydrocarbons Recovery in the Gas Rich Shales: An Insight from the Molecular Dynamics Simulations. In Proceedings of the Carbon Management Technology Conference, Sugar Land, TX, USA, 17–19 November 2015. CMTC-439481-MS. [CrossRef]
15. Wang, S.; Feng, Q.; Zha, M.; Lu, S.; Qin, Y.; Xia, T.; Zhang, C. Molecular dynamics simulation of liquid alkane occurrence state in pores and slits of shale organic matter. *Pet. Explor. Dev.* **2015**, *42*, 844–851. [CrossRef]
16. Haghshenas, B.; Qanbari, F.; Clarkson, C.R. Simulation of Enhanced Recovery using CO_2 in a Liquid-Rich Western Canadian Unconventional Reservoir: Accounting for Reservoir Fluid Adsorption and Compositional Heterogeneity. In Proceedings of the SPE Unconventional Resources Conference, Calgary, AB, Canada, 15–16 February 2017. SPE-185069-MS. [CrossRef]
17. Liu, Y.; Ma, X.; Li, H.A.; Hou, J. Competitive adsorption behavior of hydrocarbon(s)/CO_2 mixtures in a double-nanopore system using molecular simulations. *Fuel* **2019**, *252*, 612–621. [CrossRef]
18. Zhu, C.; Qin, X.; Li, Y.; Gong, H.; Li, Z.; Xu, L.; Dong, M. Adsorption and dissolution behaviors of CO_2 and n-alkane mixtures in shale: Effects of the alkane type, shale properties and temperature. *Fuel* **2019**, *253*, 1361–1370. [CrossRef]
19. Tovar, F.D.; Eide, O.; Graue, A.; Schechter, D.S. Experimental Investigation of Enhanced Recovery in Unconventional Liquid Reservoirs using CO_2: A Look Ahead to the Future of Unconventional EOR. In Proceedings of the SPE Unconventional Resources Conference, Society of Petroleum Engineers, The Woodlands, TX, USA, 1–3 April 2014. SPE-169022-MS. [CrossRef]
20. Alharthy, N.; Teklu, T.; Kazemi, H.; Graves, R.; Hawthorne, S.; Braunberger, J.; Kurtoglu, B. Enhanced oil recovery in liquid–rich shale reservoirs: Laboratory to field. *SPE Res. Eval. Eng.* **2015**, *21*, 137–159. [CrossRef]
21. Le, T.; Striolo, A.; Cole, D.R. CO_2–C_4H_{10} Mixtures Simulated in Silica Slit Pores: Relation between Structure and Dynamics. *J. Phys. Chem. C* **2015**, *119*, 15274–15284. [CrossRef]
22. Xiong, F.; Rother, G.; Tomasko, D.; Pang, W.; Moortgat, J. On the pressure and temperature dependence of adsorption densities and other thermodynamic properties in gas shales. *Chem. Eng. J.* **2020**, *395*, 124989. [CrossRef]
23. Yang, Y.; Liu, J.; Yao, J.; Kou, J.; Li, Z.; Wu, T.; Zhang, K.; Zhang, L.; Sun, H. Adsorption behaviors of shale oil in kerogen slit by molecular simulation. *Chem. Eng. J.* **2020**, *387*, 124054. [CrossRef]